Journal of Materials Processing Technology 148 (2004) 93–102

Journal of Materials Processing Technology

www.elsevier.com/locate/jmatprotec

Rapid prototyping of 4043 Al-alloy parts by VP-GTAW

Huijun Wang, Wenhui Jiang, Jiahu Ouyang, Radovan Kovacevic*

Department of Mechanical Engineering, Research Center for Advanced Manufacturing, Southern Methodist University, 1500 International Parkway, Suite 100, Richardson, TX 75081, USA

Received 1 September 2003; received in revised form 21 January 2004; accepted 22 January 2004

Abstract

This paper presents an investigation on the microstructure and property of 4043 Al-alloy parts built using a novel layer-deposition technique based on a variable polarity gas tungsten arc welding (VP-GTAW) process. Processing parameters strongly affect the geometry, microstructures, roughness, and hardness of a deposited part. A hollow cylindrical part with 120 layers is built up with a good surface quality. The deposited layers have a fine dendrite structure at the top layer, and coarse columnar/cellular grain structures in the middle and at the bottom of a deposited wall. The deposited wall has some fine equiaxed grains at the surface layers of the sidewalls. The precipitates are primarily distributed at the interdendrite regions and grain boundaries. The bonding zone exhibits an epitaxial and columnar grain growth from the original grains of a substrate. Precipitates are mainly located at the interior of columnar grains in the bonding zone. The deposited wall exhibits slight increasing trend in hardness from the bottom and middle layers to the top layer. The surface roughness resulting from the fine interlayer striations is found to be in the order of 5 μm, while the verticality of sidewalls mainly depending on the surface ripples is less than 5%.

Keywords: Rapid prototyping; Al alloy; Gas tungsten arc welding; Layer deposition; Microstructure

1. Introduction

Successfully responding to the ever changing and continually increasing high demands of today's global markets requires the rapid product development and manufacturing of new designs. Over the past decade, solid freeform fabrication (SFF) has gained popularity worldwide because of the capability of significantly impacting the length of time between the initial concept and actual part fabrication. The following terms are often used interchangeably when referring to SFF technology: rapid prototyping/manufacturing, desktop manufacturing, layered manufacturing, and tool-less manufacturing. The key idea of SFF is an additive layered manufacturing paradigm that maps complex three-dimensional geometry into simple 2.5-dimensional representations, without part-specific fixturing or tooling. The turnaround time for a typical SFF part can be a few days. Conventional prototyping may take weeks or even months. Other advantages offered by this technology include the capability to produce components with small internal cavities and greater geometric complexity, ease of automatic planning, and smaller lot sizes than offered by conventional fabrication methods. Current SFF techniques (stereolithography, selective laser sintering, laminated object manufacturing, fused deposition manufacturing, and three-dimensional printing) can produce prototypes made from wax, plastic, nylon, polycarbonate materials, metals, and ceramics. However, metallic parts with good surface quality, accurate dimensions, and high structural strength cannot be produced directly with the rapid prototyping techniques. Industry has expressed a very strong interest to further develop current prototyping techniques or create new ones that are capable of directly producing metallic or ceramic parts. The transition from polymers to metals and ceramics is just beginning to take place. There are many more difficulties associated with producing a structurally sound, dimensionally accurate metallic part rather than simply a tangible three-dimensional model for visualization purposes. But if achieved, metallic parts will offer several advantages over plastic parts such as high strength, great impact resistance and toughness, and great durability [1]. Typically, metallic parts can be accomplished through selective laser sintering, brazing (soldering), arc welding deposition, laser deposition, and electron beam deposition.

The use of welding to create freestanding shapes was established in Germany in the 1960s [2]. Companies such as Krupp, Thyssen, and Sulzer developed welding techniques

* Corresponding author. Tel.: +1-214-768-4865; fax: +1-214-768-0812.
E-mail address: kovacevi@engr.smu.edu (R. Kovacevic).

0924-0136/$ – see front matter © 2004 Elsevier B.V. All rights reserved.
doi:10.1016/j.jmatprotec.2004.01.058

for the fabrication of large components of simple geometry such as pressure vessels that can weigh up to 500 t [3]. Other work in this area was undertaken by Doyle et al. [4] who worked mainly on large components produced in an austenitic material. Also, work by Rolls-Royce centered on investigating the technique as a means of reducing the waste levels of expensive, high-performance alloys that can occur in conventional processing. Rolls-Royce successfully produced various aircraft engine parts in nickel-based and titanium-based alloys. Research work on the weld-based RP continues at the University of Nottingham, UK [5], the University of Minho, Portugal, the University of Wollongong, Australia [6], and Southern Methodist University, USA [7,8]. Two new research groups, one from Korea [9] and the other consisting of researchers from the Indian Institute of Technology Bombay and the Faunhofer Institute of Production Technology and Automation [10], presented their conceptual ideas of combining a welding operation with milling. The Korean research group proposed to combine welding and 5-axis CNC milling for the direct prototyping of metallic parts. The other research group from Germany and India proposed to combine welding with 2.5-axis milling, where the complex shapes of the layers are obtained by using cutters with specific geometry. The brazing process is proposed to deposit the masking material at the edge of each layer in order to allow the formation of an overhang [11]. Previous rapid prototyping techniques have produced either steel parts or non-metallic physical models that do not have the properties of functional parts. Because many important parts are made of aluminum alloys, the development of a rapid prototyping technique that can produce functional parts of aluminum alloys is an important research goal.

2. Experimental procedure

Rapid prototyping of the 4043 Al-alloy was carried out using VP-GTAW equipment with a tungsten electrode 3.2 mm in diameter, as shown in Fig. 1. The Z'-axis holding the weld torch was fixed to the Z-axis. The traveling speed of the Z-axis depended on the height of the deposited layer and the rotational speed of a substrate. The motion along the Z'-axis was monitored and controlled to provide a constant arc length during the deposition process according to the acquired arc-length signal. A 6061-T6 Al-alloy plate fixed on a rotating R-axis was used as the substrate to build up three-dimensional parts, as shown in Fig. 1. Three key factors are substrate preheating, arc length monitoring and controlling, and heat input controlling [11]. The relevant experimental conditions were selected as shown in Table 1.

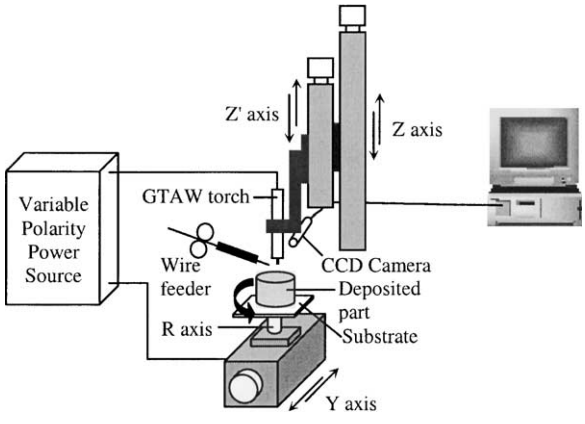

Fig. 1. Experimental set-up.

Table 1
Experimental condition for rapid prototyping of 4043 Al-alloy

Welding speed (mm/s)	60–100
Arc current (A)	110–180
Arc length (mm)	3
Electrode material	Tungsten
Electrode diameter (mm)	3.2
Diameter of welding wire (mm)	1.2
Gas flow of argon (l/min)	10
Type of torch	Straight torch, water cooled

The following analyses are performed to compare the specimens resulting from different studies: microhardness testing for selected samples, microstructure and porosity evaluation for all samples, surface roughness for selected samples, and deposit width and height for selected samples. The microhardness testing is performed using a Vickers microhardness tester and a 200 g load for 10 s duration on polished specimens. For microstructural observations, all samples are etched using a modified Keller's reagent, then observed using an optical microscope. A surface texture-measuring device is used to study the surface roughness. The maximum profile roughness height is the distance between the lowest and highest points on a micro-scale surface. The verticality of deposited sidewalls is evaluated on a macro-scale through the calculation of the relative error in width, which is defined as the percentage of a difference between the maximum and the minimum-layer width divided by the designed-layer width.

3. Results and discussion

3.1. Effect of processing parameters on the geometry of deposited layers

The processing parameters in VP-GTAW include the arc voltage (arc length), welding current, welding speed, and wire-feeding rate. The amount of energy produced by the arc is directly proportional to the current and voltage. The amount of energy transferred per unit length of weld is inversely proportional to the welding speed. However, because these parameters interact strongly, it is difficult to treat them as completely independent variables when establishing a welding procedure for fabricating specific deposits.

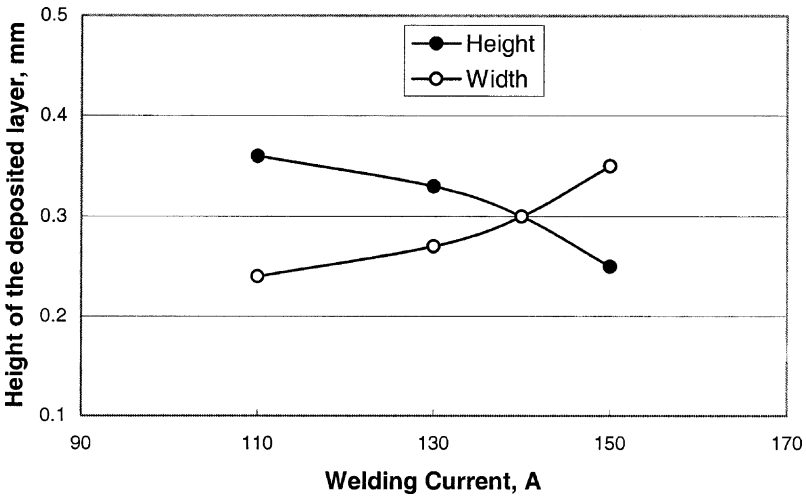

Fig. 2. Effect of welding current on the geometry of deposited layers.

Numerous single-pass layers are produced in the experiments to decide the optimized parameters and their effects on the geometry of the deposited layers. Optimizing the parameters allows the deposit of both single and continuous layers instead of discontinuous bonded droplets on the substrate. Fig. 2 shows the effect of the welding current on the geometry of the single-pass deposited layers at a 3 mm arc length, 80 mm/s welding speed and 100 mm/s wire-feeding rate. The height of the deposited layer decreases with an increase in the welding current from 110 to 150 A. However, the width of the deposited layer exhibits an increasing trend with an increase in the welding current from 110 to 150 A. The heat input is directly proportional to the product of welding current and arc voltage. Therefore, the width of the deposited layer increases with an increase in the heat input. The arc current also influences the weld penetration with the effect being proportional.

The effect of the welding speed on the geometry of the single-pass deposited layers under the welding conditions of a 3 mm arc length, 140 A welding current, and a 100 mm/s wire-feeding rate is shown in Fig. 3. It can be seen that both the height and width of the deposited layer decrease with an increase in the welding speed from 60 to 100 mm/s, such that the effect on the width is more pronounced than on the height. For example, the height decreases only to 0.25 mm, whereas, the width decreases to 2.1 mm. A welding speed is an important factor. Decreasing a welding speed also increases the penetration and flattens the contour of deposited layers. Higher welding speeds are preferred to achieve production efficiency, a good quality of deposited products.

Fig. 4 shows the effect of a wire-feeding rate on the geometry of single-pass deposited layers at a 3 mm arc length, a 140 A welding current, and a 80 mm/s welding speed. The height of the deposited layers increases with an increase in the wire-feeding rate from 80 to 130 mm/s. However, the situation is reversed for the effect of a wire-feeding rate on the width of the layers. It should be noted that the variations in the feeding rates of a filler metal applied to a weld may result in different arc lengths and, hence, different arc

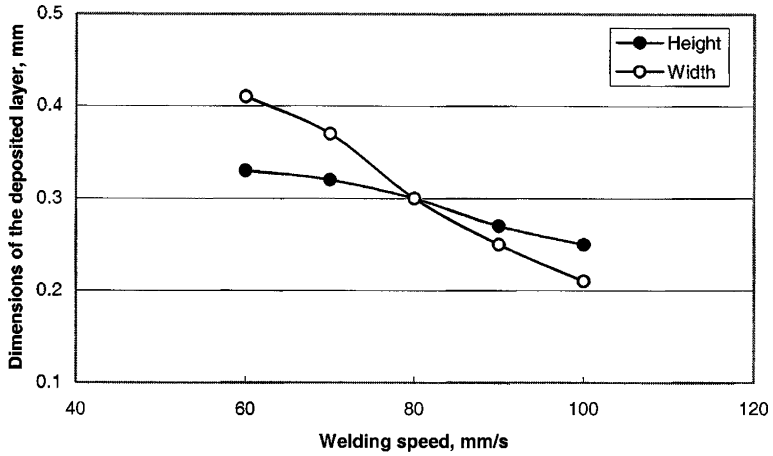

Fig. 3. Effect of a welding speed on the geometry of deposited layers.

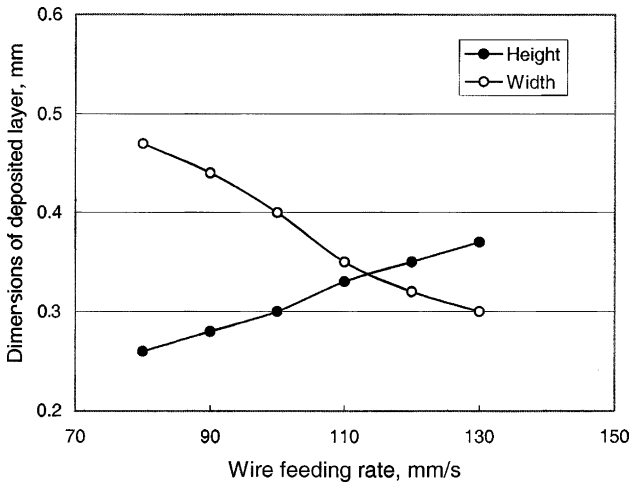

Fig. 4. Effect of a wire-feeding rate on the geometry of deposited layers.

voltages. That variation directly affects the heat input and, thus, an arc length control is necessary to eliminate this effect. The higher the wire-feeding rate, the more the welding arc energy is needed to melt the filler metal. This effect may result in a lack of substrate fusion and lead to a decrease in the width of the layers. A wire-feeding rate influences the number of passes required and the appearance of the deposited layers. Increasing the wire-feeding rate decreases weld penetration and produces a more convex clad layer.

The geometry of deposited layers depends on welding parameters. Welding current, welding speed and wire-feeding rate are the most important affecting factors. An amount of work demonstrated that a deposited layer with a similar geometry can be achieved by different combination of these processing parameters. Some typical buildups of deposited parts are examined as follows.

3.2. Buildup of layered-structures

The high quality layered structures depend on the metallurgical bonding developed by re-melting the thin layer of a previously deposited layer, controlling the cooling rate, and minimizing the residual stress. Fig. 5 shows the cross-sections and surface morphologies of deposited layers with one, two, and eight passes under the welding conditions of a 140 A welding current, a 3 mm arc length, a 80 mm/s welding speed, and a 100 mm/s wire-feeding rate. A good metallurgical bonding was developed by melting a filler metal and the thin layer of a substrate. Metallographic examinations do not detect any defects in the deposited layers or at the interface. From the second layer, the molten filler metal solidifies in contact with the previous layer. The contact by the liquefied material causes the previous layer to be partially re-melted, thereby, ensuring a good metallurgical bonding between layers. A similar situation occurs in the successive layers.

Fig. 6 illustrates the typical morphology of a hollow cylindrical 4043 Al-alloy part under the welding conditions of a 100–140 A welding current, a 3 mm arc length, a 80 mm/s welding speed, and a 100 mm/s wire-feeding rate. This cylindrical part, consisting of 120 overlaid helical layers of a single-bead wall thickness, is built on the substrate of a 6061-T6 Al-alloy. It is demonstrated that more heat input is needed for the first several layers so as to obtain a good wetting on the substrate. The heat is constantly accumulated in a deposited layer until a balance between the heat input and dissipation to previously deposited layers and to the environment is achieved. Since this accumulation of heat influences the deposited morphologies and structures, adjusting the processing parameters is necessary depending on the height. An effective way to control the dimension of deposited products is to reduce gradually the heat input during a process. The

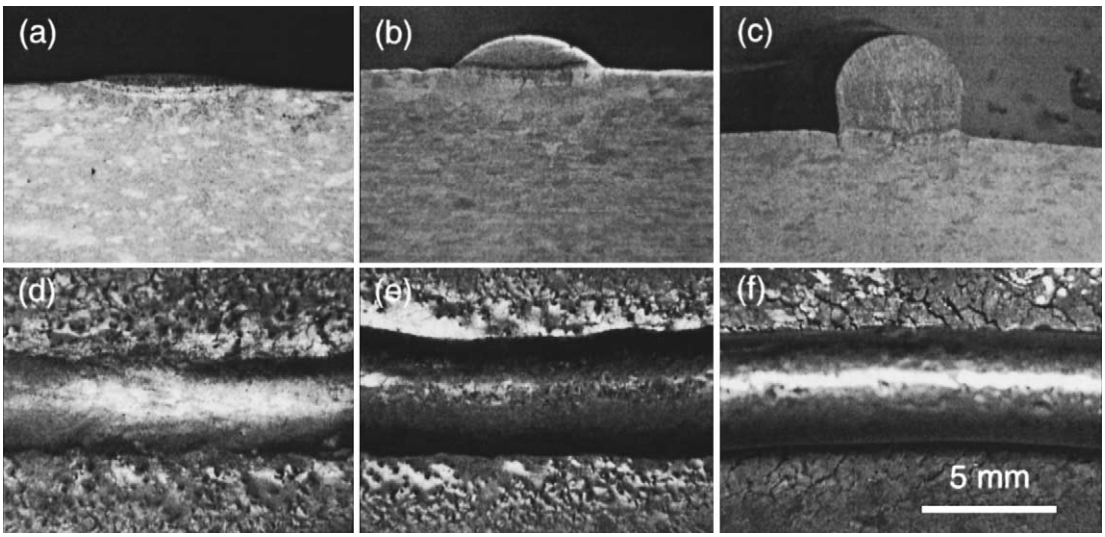

Fig. 5. Cross-sections (a–c) and surface morphologies (d–f) of deposited layers with various passes: (a) and (b) single layer; (c) and (d) double layers; (e) and (f) eight layers.

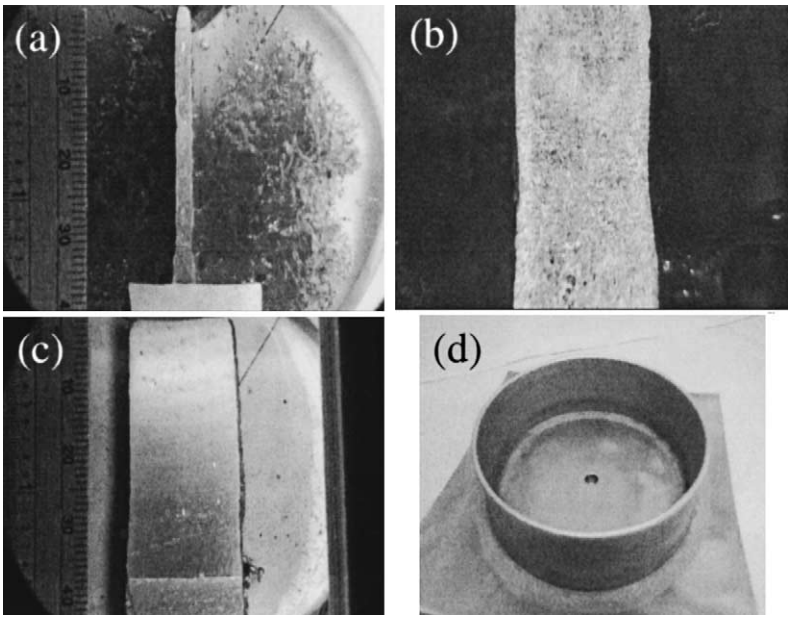

Fig. 6. Typical morphology of cylindrical 4043 Al-alloy parts, consisting of different overlaid helical layers: (a) cross-section of a 120-layer wall; (b) enlarged morphology of localized surface undulations resulting from arc instabilities; (c) longitudinal section of a 120-layer wall; (d) a 120-layer cylindrical part.

control of heat input is realized by reducing a welding current from 140 to 100 A in the first 40 layers with a decreasing step of 1 A per layer and keeping it constant at 100 A for the rest of the layers. The part is created layer-by-layer as shown in Fig. 6(d). The metallographic observations show that the cylindrical part exhibits a good structural integrity and a good bonding between the deposited layers.

The surface morphology of the sidewalls of the deposited cylindrical parts with and without heat input control is shown in Fig. 7. From Fig. 7(a), fine striations are observed at the surface of the sidewalls with heat input control. These fine striations are indicative of the typical patterns of interfaces caused by layered deposition. Only a very few surface ripples with a low amplitude are found at the surface of the deposited part with heat input control (see also Fig. 6(b)). However, from Fig. 7(b) both fine striations and coarse periodic ripples are observed at the surface without heat input control during processing. The average spacing of the periodic surface ripples is about 3.0 mm. There are several reasons for producing the surface undulations on the sidewalls: (1) a heat buildup may cause re-melting of previously deposited layers, and lead to the distortion or collapse of a deposited structure; (2) an inaccuracy in welding variables may cause cumulative errors; (3) a filling in of outline shapes, solid layer, cannot be performed with sufficient accuracy to form a smooth surface. The excessive accumulation of heat, depending on the height, influences the layer width and produces a distinct surface relief. Progressive solidification along the height direction gives rise to the formation of coarse periodic ripples on a macro-scale. An arc length is also important during this process because it affects the width of a molten pool. In this experiment, the arc length is kept at a given value of 3 mm.

3.3. Microstructural observations

The microstructures in the deposited layers, the bonding zone, and the heat-affected zone of the substrate have been investigated in this section. In order to understand the

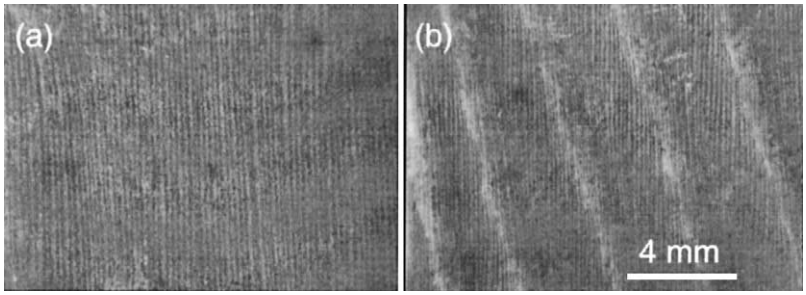

Fig. 7. Surface morphology of the sidewalls of the deposited cylindrical parts: (a) fine striations on the surface with heat input control; (b) fine striations and coarse periodic surface ripples without heat input control during the deposition.

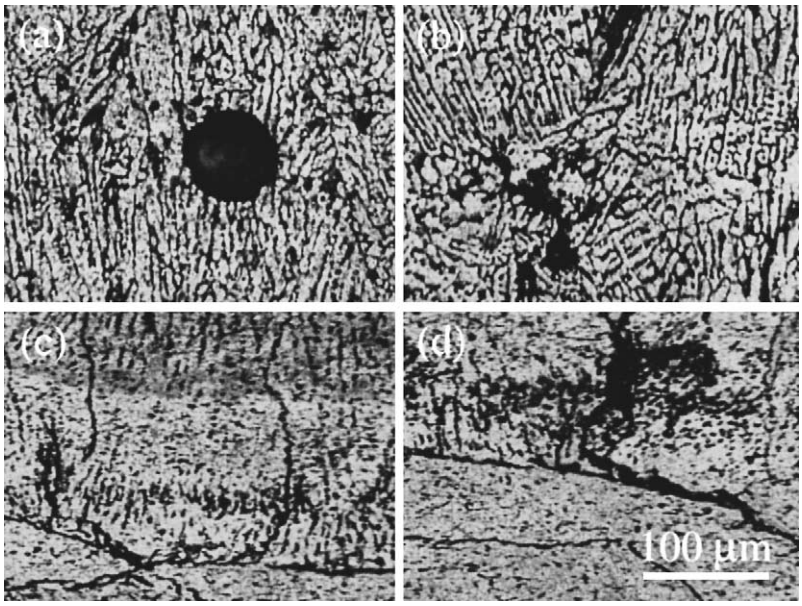

Fig. 8. Microstructures of the top layer of 4043 Al-alloy part: (a) microstructural transition at the top layer; (b) microstructural feature and precipitates at the upper region in (a); (c) higher magnification of fine dendrites at the upper region; (d) higher magnification of coarse dendrites at the lower region in (a).

development of structures and properties in a deposited wall, it is important to know about the thermal gradient and cooling rate in and around the molten pool. The cooling rate controls the morphology and scale of a solidified structure and is the primary factor in determining the properties of a deposited part. The microstructures of the deposited 4043 Al-alloy are complex and highly dependent on their locations in deposited layers where different heating and cooling rates are experienced during processing. Fig. 8 shows the microstructures at the top layer of the deposited 4043 Al-alloy part. A distinct microstructural transition is observable. The upper region exhibits a fine dendrite structure, while the lower region has a coarse dendrite structure. Since the uppermost layer of the deposited wall has hardly been affected by the heat, the grains are much finer. Precipitates are primarily distributed at the interdendritic regions. At the upper region, the average spacing of the secondary dendrite arms is about 4 μm, as shown in Fig. 8(c). At the lower region, however, it is about 8 μm, as shown in Fig. 8(d). The size of grain structures is closely related to the cooling rate. Rapid cooling at surface layers yields finer grains, while slow cooling at the lower region results in coarser grains. Fig. 9 shows the microstructures in the middle and bottom of the deposited part. Within the interior of the deposited layer, the grains mostly exhibit a more cellular structure with precipitates distributed at the interdendritic regions and grain boundaries, as shown in Fig. 9(b). An oriented grain structure (see Fig. 9(a)) may be attributed to directional cooling, and the direction of the grain growth must be along the largest temperature gradient during solidification. As the direction of heat flowing is mainly along the deposited parts towards the substrate, the primary dendrites are very long, slender, and perpendicular to the substrate. The average spacing of the cellular grains or primary dendrite arms is around 7–10 μm. At the surface layers of the sidewalls, the equiaxed grains are developed because of relatively rapid cooling. Fig. 9(c) and (d) shows that the equiaxed grains at the inside wall of the cylindrical part are slightly larger than those at the outside wall, which is caused by a difference in a cooling rate.

A cooling rate during solidification can be determined with a secondary dendrite arm spacing or mean intercept length of cell boundaries. The relationship between the spacing of cellular grain or secondary dendrite arm and the cooling rate can be expressed with the following empirical formulate [12,13]:

$$\lambda_2 = B\varepsilon^{-n}$$

where λ_2 is the spacing of cellular grain or secondary dendrite arm, ε the cooling rate, and B and n are material and process dependent constants. For Al alloys, they are typically about 50 μm $(\mathrm{K\,s^{-1}})^n$ and 1/3, respectively, over the range of about 10^{-5} to $10^6\,\mathrm{K\,s^{-1}}$ [13]. The λ_2 is determined by taking an average value of the cellular grain or secondary dendrite arm spacing from the deposited layer in the center of the samples.

In a deposited layer, a secondary dendrite arm spacing changes with location indicating that the cooling rate varies. In some regions, secondary dendrite arms could not be found, therefore, the average spacing between the cellular grains was used to evaluate the cooling rate. The cellular grains and the primary dendrites have similar spacing at the bottom of the deposited layer. Measurement and calculation indicate that in the present experiment, the cooling rate varies from 10^2 to $10^3\,\mathrm{K\,s^{-1}}$ depending on the location in the deposited part. The highest cooling rate is at the top layer of the deposited part. The cooling rates in rapid

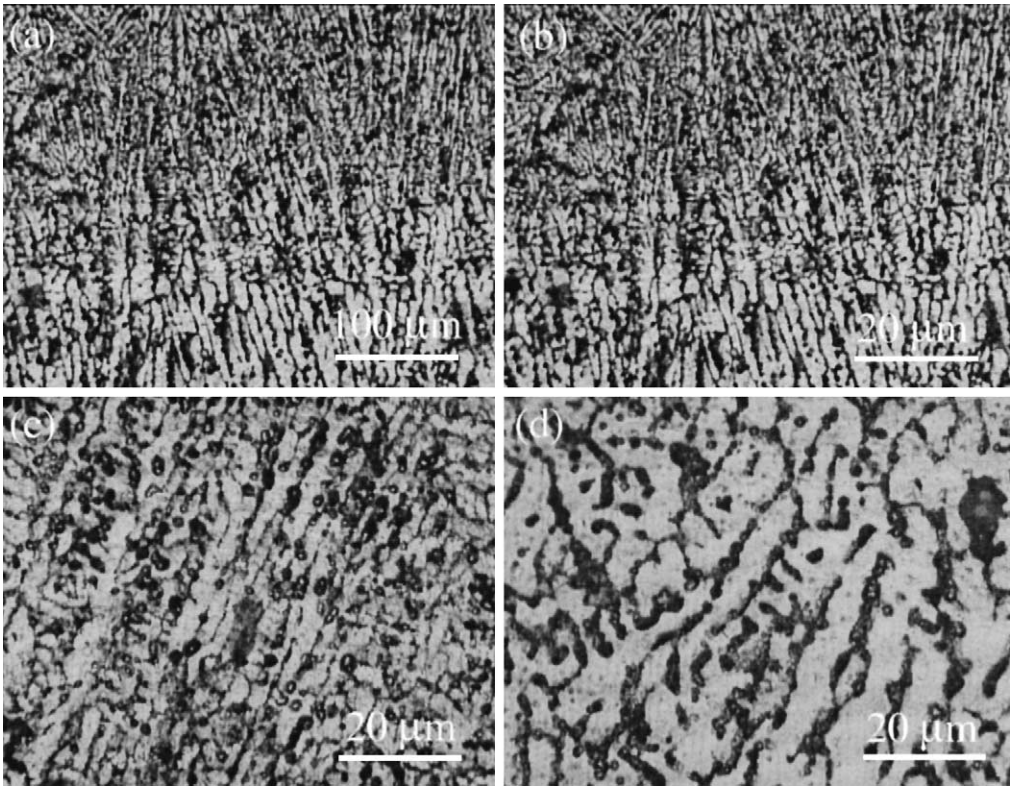

Fig. 9. Microstructures of the deposited layers of 4043 Al-alloy: (a) an oriented growth in the middle or bottom part of the deposited layer; (b) precipitates at the grain boundaries; (c) equiaxed grains at the inside wall of the part; (d) equiaxed grains at the outside wall of the part.

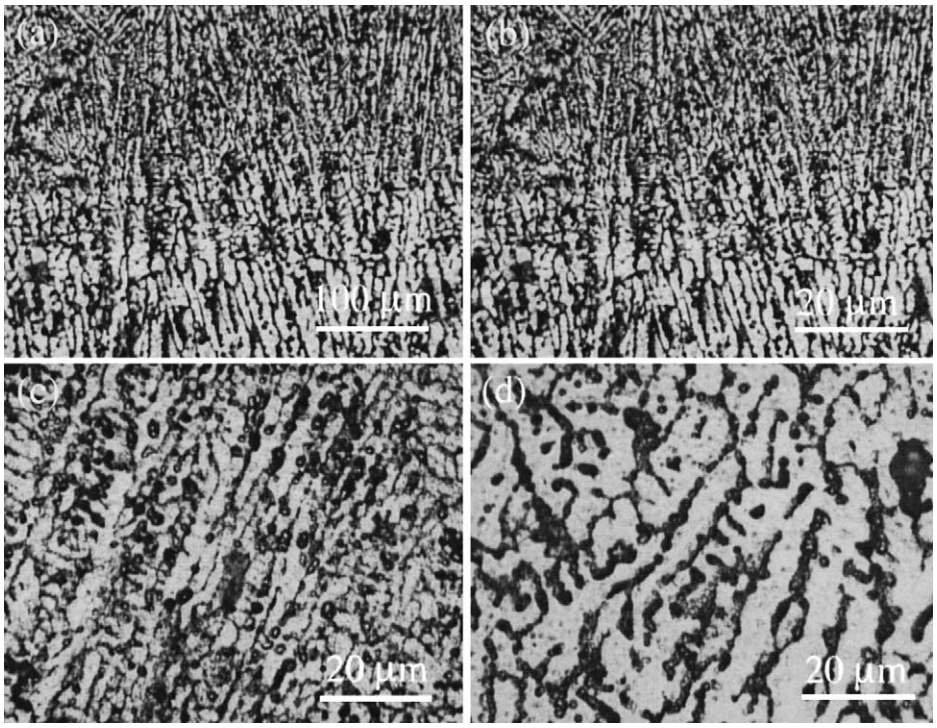

Fig. 10. Microstructures of the bonding zone between the deposited wall and the substrate: (a) morphology of the bonding zone; (b) coarse columnar grain grown epitaxially from the original grain boundaries; (c) and (d) distribution of precipitates in the interior of columnar grains; (e) transition from the columnar grains of the bonding zone to the fine equiaxed grains of the deposited wall.

prototyping are higher than those in a traditional fusion welding process. It should be noted that the spacing of the secondary dendrite arms used for the calculation is an average value of several measurements.

The microstructures in the bonding zone shown in Fig. 10 contain partially melted grains and the epitaxial columnar grain growth from the original grain boundaries of the 6061-T6 Al-alloy substrate. The initial growth starts epitaxially from the partially melted grains (Fig. 10(e)). The direction of grain growth is approximately perpendicular to the solid/liquid interface and is along the direction of the heat flow. There are two different types of precipitates observed in the bonding zone. One is distributed along the fine columnar grain boundaries, and the other is located around the coarse grains. The compositional changes associated with an addition of the 4043 Al-alloy may be an important factor.

The heat-affected zone has the maximum temperature below the melting point of 6061-T6 Al-alloy where no melting occurs. However, many solid-state reactions such as grain growth and coarsening of precipitates occur in this zone. Undoubted, such a reaction may affect the properties of the deposited part. For the heat treatable 6061-T6 Al-alloy, the dissolution of the strengthening phase β'' (semicoherent rods of Mg_2Si), and formation and growth of the non-strengthening phase β' cause softening in the heat-affected zone. The microstructure of the 6061-T6 Al-alloy substrate is shown in Fig. 11. The grains of the alloy are elongated along the rolled direction.

3.4. Microhardness and surface roughness

The microhardness of a deposited part is found to slightly vary depending on location, which is attributed to different

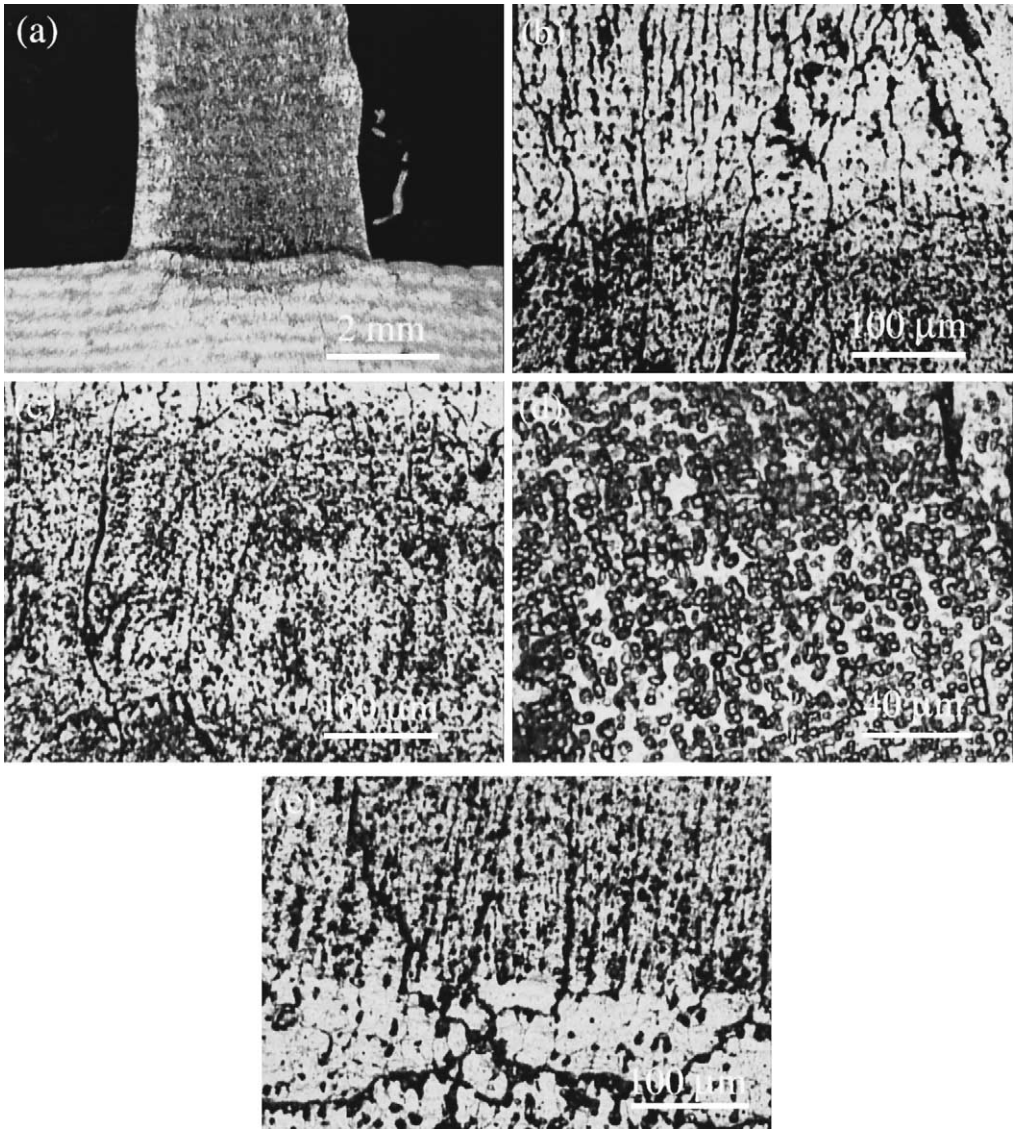

Fig. 11. Microstructures of the 6061-T6 Al-alloy substrate: (a) the elongated grains along the rolled direction; (b) the precipitates.

microstructures. The hardness values of the fine dendrites and coarse columnar/cellular dendrites of the deposited wall are typically 42–51 $HV_{0.2}$. All the hardness values are taken from an average of at least three measurements in the same region. In order to show the variations of the hardness values over a whole sample, three arrays of the measurements are taken along the centerline of the deposited layers. The hardness is the smallest (32–39 $HV_{0.2}$) in the bonding zone, increases gradually towards the bottom and intermediate (40–44 $HV_{0.2}$), and reaches the maximum (45–51 $HV_{0.2}$) at the top layer of the deposited wail. The bottom layer of the deposited wall is softer than the top layer because the bottom layer is softened by excessive exposure to heat. The hardness of the heat-affected zone of the substrate is about 55–60 $HV_{0.2}$.

The surface roughness of a deposited wall is found to relate to the direction along which the measurements are taken with respect to the welding. In examining the surface roughness, four directions are examined for each sample: both parallel and perpendicular to the welding direction on the top surface, and the horizontal and vertical directions on both the outside and inside of the walls. It is found that the roughness in the vertical direction on the sidewall is distinctly greater than the horizontal direction. At the top surface, the roughness perpendicular to the welding direction is much greater than the roughness parallel to the welding direction. Since the largest roughness on each sample is particularly of interest, the results are compared only in the vertical direction on the sidewalls. If a heat input is not controlled, the surface undulations of a deposited wall are found to be directly related to the thickness of the wall. As the wall becomes thicker, the periodic surface ripples with a spacing of 3 mm, as shown in Fig. 8(b), are formed on the sidewall. The heat input control is realized by reducing the welding current in the first 40 layers with a decreasing step of 1 A per layer, then keeping the welding current at the level of 100 A for the rest of the layers. The arc length control is applied to keep a given value of 3 mm during the deposition process. Only a very few surface ripples are found on the surface of the deposited part with heat input control. The designed cylindrical part consists of 120 overlaid helical layers with a layer height of 0.3 mm, a layer width of 3.0 mm, and a diameter of 110.0 mm. The resulting part is 36.5 mm in height, 2.85 mm in width, 108.7 mm in diameter, and 1.4% in the error of the part height, 5% in the error of the part width, and 1.1% in the error of the part diameter. The average of the surface roughness R_a is 4.67–5.44 μm. As for verticality of the deposited wall, at present the accuracy is about 5%, and it is expected that it will be reduced eventually to 2% by monitoring welding variables so as to reduce the amplitude of surface ripples. Despite the inherent surface undulations resulting from arc instabilities, this geometry-controlled VP-GTAW process can be used for rapid prototyping of the fully dense prototypes of a 4043 Al-alloy.

4. Conclusions

Rapid manufacturing based on a variable polarity gas tungsten arc welding offers a novel route to produce a three-dimensional part of an Al-alloy. Processing parameters strongly affect the geometry, microstructures, roughness, and hardness of a build up. A hollow cylindrical part with 120 layers of 4043 Al-alloy is built up with a good surface quality. The deposited layers have a fine dendrite structure at the top layer, coarse columnar/cellular grain structures in the middle and at the bottom of a deposited wall. The deposited wall has some fine equiaxed grains at the surface layers of the sidewalls. The precipitates are primarily distributed at the interdendrite regions and grain boundaries. It is estimated that a cooling rate varies from 10^2 to 10^3 K s^{-1} depending on location The highest cooling rate is at the top layer of the deposited wall. The bonding zone exhibits an epitaxial and columnar grain growth from the original grains of a substrate. Precipitates are mainly located at the interior of the columnar grains in the bonding zone. The deposited wall exhibits a slight increasing trend in hardness from the bottom and middle layers to the top layer. The surface roughness resulting from the fine interlayer striations is found to be in the order of 5 μm, while the verticality of sidewalls mainly depending on the surface ripples is less than 5%.

Acknowledgements

The authors would like to give their gratitude to Mr. M. Valant for technical support. This work was financially supported by THECB's Grant Nos. 003613-0005-1997 and 003613-0022-1999, NSF's Grant Nos. DMI-9732848 and DMI-9809198, and by the US Department of Education Grant No. P200A80806-98.

References

[1] R. Kovacevic, Rapid manufacturing of functional parts based on deposition by welding and 3D laser cladding, in: Proceedings of the Mold Making 2001 Conference, Rosemont, IL, April 2001, Presented by Mold Making Technology Magazine, 2001, pp. 263–276.

[2] K. Kassmaul, F.W. Schoch, H. Lucknow, High quality large components 'shape welded' by a SAW process, Weld. J. 62 (9) (1983) 17–24.

[3] K.-H. Piehl, Formgebendes Schweißen von Schwekomponenten, Company Report: Thyssen Aktiengesellschaft, Duisburg, January 1989.

[4] T.E. Doyle, Shape melting technology, in: Proceedings of the Third International Conference on Desktop Manufacturing: Making Rapid Prototyping Pay Back, The Management Round Table, October 1991.

[5] P.M. Dickens, M.S. Prodham, R.M. Cobb, R.C. Gibson, Rapid prototyping using 3D welding, in: Proceedings of the Third Annual Solid Freeform Fabrication Symposium, Austin, TX, August 1995, pp. 280–290.

[6] A.F. Ribeiro, J. Norrish, Rapid prototyping process using metal directly, in: Proceedings of the Seventh Annual Solid Freeform Fabrication Symposium, Austin, TX, August 1996, pp. 249–256.
[7] R. Kovacevic, H.E. Beardsley, Process control of 3D welding as a droplet-based rapid prototyping technique, in: Proceedings of the Ninth Annual Solid Freeform Fabrication Symposium, Austin, TX, August 1998, pp. 57–64.
[8] H.E. Beardsley, R. Kovacevic, Controlling heat input and metal transfer for 3D welding-based rapid prototyping, in: Proceedings of the Fifth International Conference on Trends in Welding Research, Pine Mountain, GA, June 1998.
[9] Y. Song, S. Park, K. Hwang, D. Choi, H. Jee, 3D welding and milling for direct prototyping of metallic parts, in: Proceedings of the Ninth Annual Solid Freeform Fabrication Symposium, Austin, TX, August 1998, pp. 495–502.
[10] K.P. Karunakaran, P. Shanmuganathan, S. Roth-Koch, K.U. Koch, Direct rapid prototyping of tools, in: Proceedings of the Ninth Annual Solid Freeform Fabrication Symposium, Austin, TX, August 1998, pp. 105–112.
[11] H. Wang, R. Kovacevic, Variable polarity GTAW in rapid prototyping of aluminum parts, in: Proceedings of the 11th Annual Solid Freeform Fabrication Symposium, Austin, TX, August 2000, pp. 369–376.
[12] I.C. Stone, P. Tsakiropoulos, Cooling rates in gas atomised Al–4 wt.% Cu alloy, Int. J. Rapid Solid 7 (3) (1992) 177–190.
[13] E.A. Stark Jr., in: A.K. Vasudevan, R.H. Doherty (Eds.), Aluminum Alloys: Contemporary Research and Applications, Academic Press, New York, 1989, p. 35.